American Mineralogist, Volume 83, pages 259–272, 1998

The chemical composition of REE-Y-Th-U-rich accessory minerals in peraluminous granites of the Erzgebirge-Fichtelgebirge region, Germany, Part I: The monazite-(Ce)-brabantite solid solution series

HANS-JÜRGEN FÖRSTER

Geo Forschungs Zentrum Potsdam (GFZ), Telegrafenberg, 14473 Potsdam, Germany

ABSTRACT

Peraluminous granites of the Erzgebirge-Fichtelgebirge, Germany, are hosts of various members of the monazite group of minerals that display an unprecedented compositional diversity. The Eibenstock S-type granite constitutes the third reported occurrence worldwide of brabantite and the first occurrence of this mineral in a granite. Many new occurrences of cheralite-(Ce), as well as a monazite-group mineral intermediate between monazite-(Ce) and huttonite for which the term huttonitic monazite is proposed, were discovered. Even ''common'' monazite-(Ce) may show extreme ranges of actinide and lanthanide element concentrations.

The granites that host brabantite and cheralite-(Ce) are highly differentiated, strongly peraluminous, low-temperature residual melts of S-type affinity, which are rich in fluorine and other volatile constituents but depleted in thorium and the light rare-earth elements. Such highly evolved, volatile-rich compositions resemble rare-element pegmatites and appear favorable for the precipitation of cheralite-(Ce) and brabantite, but not of monazite with large amounts of huttonitic substitution. Instead, these minerals occur preferentially in F-poor biotite and F-rich Li-mica granites of A-type affinity. Irrespective of the level of uranium in silicate melts, which may exceed that of thorium, the substitution of uranium in monazite remains limited.

The compositional data reported here are consistent with complete miscibility in the monazite-(Ce)-brabantite solid solution series under magmatic conditions. These granites contain monazites that span almost the entire compositional range reported for monazite-group minerals worldwide, and therefore granites appear to be ideal rocks in which to study the crystal chemistry of this mineral group in general.

INTRODUCTION

The light rare-earth element (LREE) phosphate mineral monazite most commonly occurs as an accessory phase in peraluminous granites, syenitic and granitic pegmatites, quartz veins, and carbonatites, as well as in charnockites, migmatites, and paragneisses (Rapp and Watson 1986). In peraluminous granites, monazite constitutes a major host for the LREE (except Eu) and the actinides thorium and uranium (Hinton and Paterson 1994; Bea et al. 1994; Bea 1996), and it commonly contains minor amounts of yttrium and the heavy rare-earth elements (HREE). The stability of monazite in silicate melts depends on numerous compositional parameters of the melt such as the activities of SiO_2, CaO, and P_2O_5, the oxygen fugacity, the peraluminosity, and the ratios and contents of the lanthanides and actinides (Cuney and Friedrich 1987; Casillas et al. 1995). Several experimental studies of monazite solubility in granitic melts have been made in the past decade (Rapp and Watson 1986; Rapp et al. 1987; Montel 1993; Wolf and London 1995). The stability of monazite and its solubility in melts control the distribution of LREE, Th, and U between melts and restite during partial fusion (Rapp et al. 1987; Watt and Harley 1993; Nabelek and Glascock 1995). The strong LREE and Th depletions commonly observed in felsic differentiates of multiphase granite plutons also may be due to monazite fractionation (Ward et al. 1992; Wark and Miller 1993; Zhao and Cooper 1993).

SHRIMP ion-microprobe measurements proved that monazite can occur as an inherited accessory mineral (Miller et al. 1992; Harrison et al. 1995) and thus may be useful for evaluating the age and nature of source material from which a silicate magma was derived. In addition to the wide use of monazite for conventional U-Pb dating (e.g., Parrish 1990), this mineral also has received renewed interest because of the potential for determining Th-U-Pb ages by electron microprobe analyses (Suzuki et al. 1994; Montel et al. 1996; Rhede et al. 1996). The monazite structure also has received considerable attention for use as a long-term solid state host for storing radionuclides (e.g., Boatner and Sales 1988).

Despite the importance of monazite outlined above, only a few systematic electron microprobe studies on

0003–004X/98/0304–0259$05.00

monazite compositions from granitic rocks have been carried out (Maruéjol et al. 1990; Ward et al. 1992; Montel 1993; Wark and Miller 1993; Casillas et al. 1995; Jennings and Rowbotham 1995; Bea 1996). Many of these did not include analyses from a sufficiently large number of individual grains to be fully representative or the analyses were incomplete. To the author's knowledge, the full spectrum of REE has only been analyzed by electron microprobe in monazites from some granites in Spain (Casillas et al. 1995). The result is that published chondrite-normalized patterns for the heavy rare-earth elements (HREE) are generally irregular and exhibit unexplainable ''anomalies'' that may be artifacts of the analyses and not characteristic of the mineral.

This paper presents results of a comprehensive electron microprobe study of monazites from geochemically diverse, multi-phase, mildly to strongly peraluminous granite plutons of the Variscan Erzgebirge-Fichtelgebirge metallogenic province in Germany. Initially aimed at the relations between monazite chemistry and melt composition, this study reveals an unprecedented range of compositions and stoichiometries previously considered as atypical for monazite from granitic environments. For example, this is the first report of brabantite from a granitic rock. This study also documents the presence of other monazite group minerals [cheralite-(Ce) and huttonitic monazite, see below] in granitic rocks, for which very few occurrences were known previously. The main objective of this paper is to present and discuss the compositional extremes of the monazite group and their relations to the geochemistry and mineralogy of their host granites and aplites. Note that about 95% of the monazites analyzed from granites have ''normal'' monazite-(Ce) compositions, and these are not described in detail.

Monazite also was found to display extreme compositional variability at a variety of scales (Förster and Rhede 1995; Bea 1996), much more so than that described from the Sweetwater Wash pluton by Wark and Miller (1993). This important feature of monazite and its geochemical implications is the subject of a forthcoming paper (H.-J. Förster, in preparation).

Geological background

The Erzgebirge-Fichtelgebirge region is situated at the northwest edge of the Bohemian Massif along the border between Germany and the Czech Republic. During the Variscan orogeny in the late Carboniferous and early Permian, this region was invaded by numerous granitic plutons of various sizes and compositions (Fig. 1) that have been described by Breiter et al. (1991), Förster and Tischendorf (1994), and Hecht et al. (1997). The granite plutons generally form composite bodies of mappable, texturally and compositionally distinct sub-intrusions that are genetically related by magmatic differentiation. The granites can be grouped into four main types according to mineralogical and geochemical criteria (Förster and Tischendorf 1994; Förster et al. 1995): (A) Biotite granites and their muscovite-bearing, aplitic differentiates (here represented by the multi-phase plutons of Kirchberg and Schlema-Alberoda); (B) two-mica granites with late, aplitic tourmaline-muscovite differentiates (here represented by the Bergen composite massif, the Schwarzenberg and Lauter plutons, and the G1S-type granite); (C) high-fluorine, high-phosphorus Li-mica granites (here represented by the Eibenstock multi-stage pluton, the buried granite occurrences of Pobershau and Satzung, and the G4-type intrusion); (D) high-fluorine, low-phosphorus biotite and Li-mica granites (here represented by the buried Seiffen granite).

The monazite compositions discussed here occur in granites of groups A and B, which possess transitional I-S type affiliation, and are particularly common in S-type granites of group C. Compositional extremes in terms of thorium concentration are also present in group D granites, which share many features of mildly peraluminous, post-collision A-type igneous rocks. Thus monazite-group minerals occur in all four granite types, and this region therefore offers an ideal chance to study the occurrence and composition of the monazite group of minerals in a wide range of granites.

Analytical methods

Mineral analyses were obtained using the CAMEBAX SX-50 electron microprobe, employing a PAP correction procedure (Pouchou and Pichoir 1985). The operating conditions were: accelerating potential 20 kV, beam current 40–60 nA (measured on the Faraday cup), and 1–2 μm beam diameter. The counting times on the peak were 300 s for Pb and 200 s for Th and U and, in each case, half that time for background counts on both sides of the peak. For the REE and other elements, counting times were 60 s and 40 s on peak, respectively.

X-ray lines and background offsets were selected to minimize interferences and their correction (Exley 1980; Roeder 1985). Wavelength-dispersive spectral scans done on complex natural REE phosphates (monazites and xenotimes) were used to determine the peak and background positions of each element and to identify overlapping peaks. *K*α-lines were used for P, Si, Fe, Ca, and F; *L*α-lines for Y, La, Ce, Yb, and Lu; and *L*β-lines for Pr, Nd, Sm, Gd, Tb, Dy, Ho, and Er. The interferences of Th*M*β on U*M*α and Y*L*α on Pb*M*α were eliminated by using the Th*M*α, U*M*β, and Pb*M*β lines. Minor interferences of Th*M*γ on U*M*β were corrected by the procedure of Åmli and Griffin (1975). The concentration of F was calculated by empirical correction for the major interference of Ce*L*α on F*K*α. The following analyzing crystals were used: LIF for REE and Fe; TAP for Si, Al, and Y; PET for P, Th, U, Ca, and Pb; and PC1 for F.

Primary standards included pure metals for Th and U (also synthetic $UO_{2.15}$), vanadinite and a synthetic glass (0.79 wt% PbO) for Pb, synthetic phosphates prepared by Jarosewich and Boatner (1991) for the REE, and natural minerals and synthetic oxides for other elements. The calibration was checked routinely using the synthetic glass

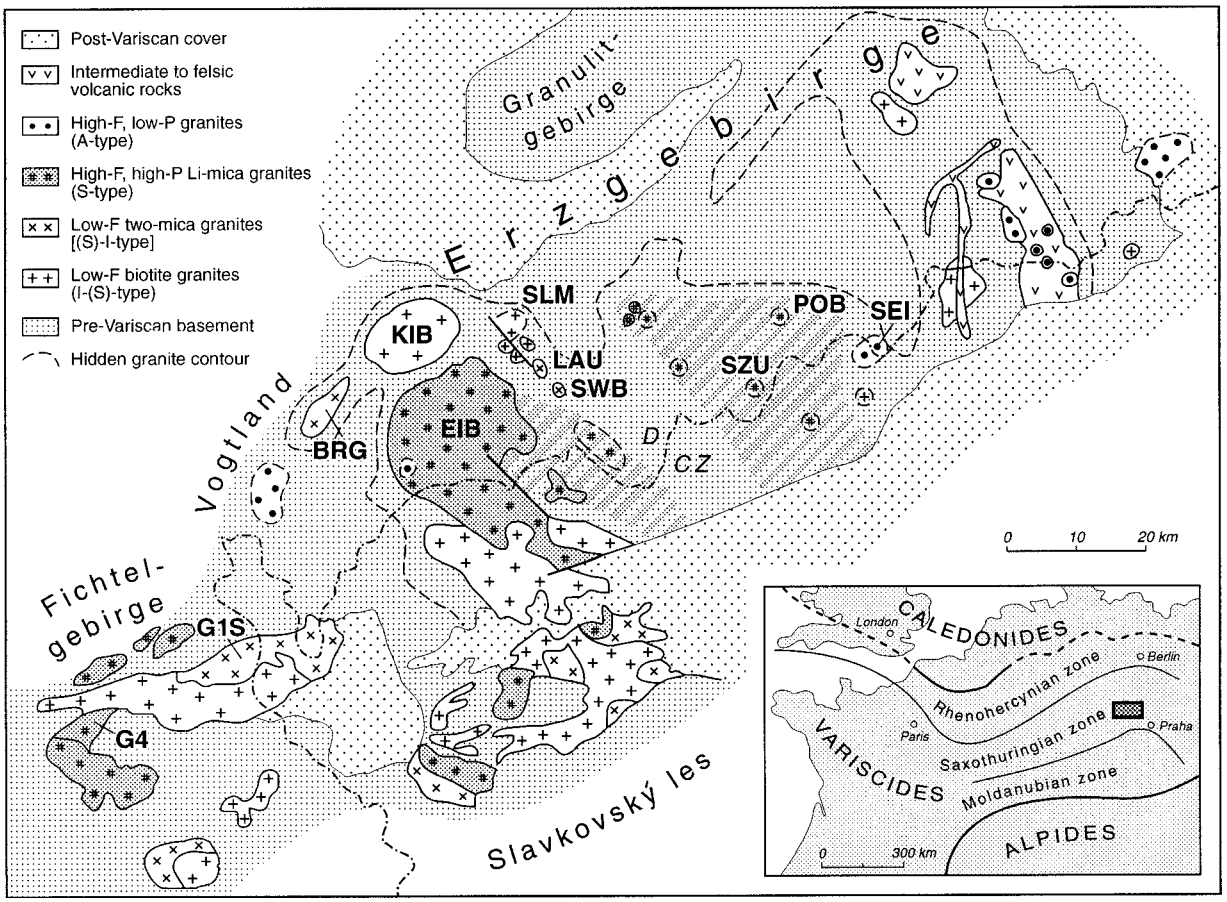

FIGURE 1. Generalized geological map of the Erzgebirge-Fichtelgebirge, showing the regional distribution of the different groups of Variscan granites and the sampled plutons. Abbreviations: BRG = Bergen, EIB = Eibenstock, KIB = Kirchberg, LAU = Lauter, POB = Pobershau, SEI = Seiffen, SLM = Schlema-Alberoda, SWB = Schwarzenberg, SZU = Satzung. The dash-dot line marks the border between Germany (D) and the Czech Republic (CZ).

SRM 610, which contains low contents of Th, U, and Pb, and the REE glasses prepared by Drake and Weill (1972).

The analytical errors for the REE depend on the absolute abundances of each element. Relative errors are estimated to be <1% at the >10 wt% level, 5–10% at the ≈ 1 wt% level, 10–20% at the 0.2 to 1 wt% level, and 20–40% at the <0.1 wt% level. The analytical uncertainties for the actinides and for lead are more uniform and amount to about 10%, even for concentrations below 0.1 wt%. Detection limits were approximately 200–300 ppm for all measured elements, except lead (≈100 ppm).

The whole-rock concentrations of the REE, Y, Th, and U in the granitic rocks were analyzed by inductively-coupled-plasma mass spectrometry (ICP-MS; Perkin-Elmer/Sciex Elan Model 500 ICP mass spectrometer). Analytical methods, precision, and accuracy are as outlined by Dulski (1994).

RESULTS

Petrographic description of monazite-group minerals

In biotite granites (group A), monazite is accompanied by apatite, zircon, thorite, and uranothorite and, especially in the more-evolved intrusions, by Th-rich uraninite and xenotime. The accessory mineral assemblages in two-mica (group B) and high-F, high-P granites (group C) are virtually identical, and include apatite, zircon, monazite, Th-poor uraninite, and xenotime. The most common REE-Y-Th-U rich accessories in the Seiffen high-F, low-P granite (group D) are monazite, zircon, and xenotime. Primary allanite-(Ce) is present only in the least-evolved sub-intrusions of the Kirchberg and Niederbobritzsch biotite granite plutons, and it is not found in the same paragenesis with monazite-(Ce).

''Normal'' monazite-(Ce) typically forms euhedral to anhedral grains of variable size (20 μm to greater than 200 μm), which may be homogeneous or compositionally zoned, and are most commonly included within biotite. In contrast, the Th- and U-rich monazite-group minerals generally occur as smaller (8–20 μm across), anhedral, partly corroded crystals, and also occur as thin rims or irregular, small domains on or in other monazite grains (Figs. 2A–2D). For example, the brabantite represented by analysis 32 in Table 1 forms a rim on a cheralite-(Ce) grain (analysis 27) (Fig. 2A). The other brabantite (anal-

TABLE 1. Electron microprobe analyses of monazite-group minerals

	Group A Biotite granites								Group B Two-mica granites			
	Monazite-(Ce)					Cheralite-(Ce)		Hutt.mo-(Ce)	Monazite-(Ce)			
Granite	SLM	KIB	KIB	KIB	SLM	KIB	KIB	KIB	SWB	G1S	BRG	LAU
Sample	1000-F	788-F	784-F	784-F	1000-F	1073-F	784-F	784-F	801-F	12506b	527-F	807-F
Mineral host	feldspar	quartz	quartz	biotite	feldspar	feldspar	feldspar	quartz	feldspar	feldspar	feldspar	biotite
Analysis	1	2	3	4	5	6	7	8	9	10	11	12
P_2O_5	30.0	22.8	29.3	29.3	30.3	28.6	29.6	13.9	30.2	29.9	22.2	30.3
SiO_2	0.25	4.93	0.86	0.68	0.36	1.37	0.70	10.7	0.34	0.19	5.18	0.19
ThO_2	—	20.8	8.39	2.24	0.45	28.1	23.5	41.8	0.15	0.78	22.2	4.87
UO_2	—	0.27	0.77	—	—	1.16	1.79	—	0.03	—	—	6.20
Y_2O_3	1.12	1.02	3.57	0.60	0.25	2.41	2.23	0.13	0.89	0.07	0.41	3.82
La_2O_3	14.6	11.4	6.32	10.0	6.15	5.91	4.52	5.56	16.2	18.0	14.1	8.59
Ce_2O_3	35.2	23.3	19.8	28.8	29.3	14.2	14.2	14.6	32.5	37.6	24.6	23.7
Pr_2O_3	3.38	2.61	3.08	3.94	5.05	1.69	2.12	1.69	3.29	3.12	2.13	2.85
Nd_2O_3	11.3	9.90	15.4	17.0	21.5	6.57	9.20	6.77	11.5	8.47	7.72	10.0
Sm_2O_3	2.19	1.60	5.28	4.54	4.34	1.85	3.15	0.80	2.35	1.04	0.82	2.86
Gd_2O_3	1.23	0.89	3.46	1.97	1.39	1.58	2.46	0.37	1.57	0.45	0.42	2.08
Tb_2O_3	0.12	0.09	0.24	0.14	0.07	0.15	0.28	0.04	0.13	0.05	—	0.20
Dy_2O_3	0.48	0.24	1.09	0.07	—	0.64	0.78	0.10	0.16	—	0.03	0.85
Ho_2O_3	—	—	0.13	—	—	0.08	0.10	—	—	—	—	0.10
Er_2O_3	0.04	0.23	0.27	—	—	0.27	0.26	0.08	0.02	—	0.05	0.39
Yb_2O_3	—	0.06	0.06	—	—	0.05	0.10	0.03	—	—	0.02	0.09
CaO	0.33	0.24	1.69	0.17	0.28	5.17	4.78	1.51	0.11	0.16	0.43	2.50
PbO	—	0.29	0.15	0.05	—	0.38	0.36	0.64	0.02	0.01	0.32	0.37
Total	100.3	100.8	100.0	99.5	99.5	100.2	100.1	98.7	99.3	99.8	100.6	99.9
Mole fractions												
$ThSiO_4$		0.197	0.034	0.020	0.004	0.053	0.027	0.426	0.001	0.007	0.210	0.007
$(La\text{-}Sm)PO_4$	0.943	0.738	0.703	0.922	0.939	0.431	0.468	0.476	0.938	0.978	0.751	0.673
$Y,(Gd\text{-}Lu)PO_4$	0.047	0.043	0.141	0.041	0.024	0.086	0.097	0.012	0.043	0.008	0.016	0.125
$(Th,Ca,U,Pb)[PO_4]_2$		0.019	0.122	0.014	0.025	0.430	0.407	0.057	0.012	0.006	0.020	0.194

Note: See Fig. 1 for explanation of the abbreviations for the sampled granites. Analysis 8 includes an additional 0.35 wt% fluorine; analyses 5 and 26 include 0.15 and 0.05 wt% FeO, resp; analyses 2 and 14 include 0.02 wt% Lu_2O_3. ''—'', analyzed but not detected. n.a., not analyzed.

ysis 33) occurs as a single, anhedral grain of 6 × 8 μm. The pitted surface of this grain probably accounts for its low analytical total of 96.6 wt%. The huttonitic monazite (Table 1, analysis 8) is included within a heterogeneously zoned, Th-rich (15–17 wt% ThO_2) monazite-(Ce) (Fig. 2C). Because of their small grain size, most Th-rich members of the monazite group do not show up well on high-resolution backscattered electron (BSE) images. However, this technique was employed routinely to locate the minerals and to ensure that all analyzed grains are devoid of recognizable inclusions of other minerals.

''Common'' monazite-(Ce) grains are commonly included in biotite, but most of the minerals discussed in this paper preferentially are hosted in quartz, feldspar, and late-crystallizing lithian micas (protolithionite and zinnwaldite). Only some of the Th-poor monazite-(Ce) grains are locally included in early biotite.

Chemical compositions and element substitutions

Table 1 presents electron-microprobe analyses for the monazite-group minerals, listed separately for biotite granites (group A), two-mica granites (group B), Li-mica S-type granites (group C), and Li-mica A-type granites (group D). The concentrations of some of the most important elements in the monazite-group minerals of this study range from nil up to the following values (all in weight percent): ThO_2 = 51.7, UO_2 = 8, Y_2O_3 = 4.7, La_2O_3 = 18.2, Ce_2O_3 = 37.6, Pr_2O_3 = 5.1, Nd_2O_3 = 21.5, Sm_2O_3 = 5.3, Gd_2O_3 = 3.5, Tb_2O_3 = 0.4, Dy_2O_3 = 1.3. The amounts of huttonite ($ThSiO_4$), monazite [$(La\text{-}Sm)PO_4$], xenotime [$(Y,(Gd\text{-}Lu)PO_4$], and brabantite [$(Th,Ca,U,Pb)(PO_4)_2$] components in the minerals range between zero and 42.6, 97.8, 15.6, and 96.8 mol%, respectively (Table 1).

Thorium. Concentrations of ThO_2 in monazite from I- and S-type granites similar to those studied here typically range from 4 to 12 wt% (Cuney et al. 1984; Jefferies 1985; Friedrich and Cuney 1989; Ward et al. 1992; Montel 1993; Wark and Miller 1993; Casillas et al. 1995; Jennings and Rowbotham 1995; Montel et al. 1996; Bea 1996). Concentrations of ThO_2 in monazites from metaluminous to mildly peraluminous F-rich granites of A-type affinity range to lower values, on the order of 1.5 to 2 wt% (Charoy and Pollard 1989; Johan and Johan 1993). The present study discovered several monazite grains in biotite-, two-mica-, and A-type granites that contain even lower amounts of ThO_2, <1 wt% (Table 1, analyses 1, 9, 10, 34). Analysis 1 in Table 1 may be the first record of a granitic monazite-(Ce) with thorium (and uranium) below the microprobe detection limit. However, Th-rich monazites are more common, and these give way to huttonitic monazite-(Ce), cheralite-(Ce), and brabantite (see Fig. 6b). In a (Th + U + Si) vs. (REE + Y + P) diagram (Fig. 3), most of the monazite analyses (marked by open

TABLE 1—*Extended*

Group B Two-mica granites			Group C Li-mica S-type granites								
Cheralite-(Ce)			Monazite-(Ce)			Cheralite-(Ce)					
G1S 11389 quartz 13	SWB 803-F feldspar 14	LAU 807-F quartz 15	POB 902-F Li-mica 16	SZU 935-F feldspar 17	EIB 814-F feldspar 18	POB 902-F Li-mica 19	SZU 924-F Li-mica 20	SZU 930-F quartz 21	G4 4194 quartz 22	G4 4194 quartz 23	G4 4194 quartz 24
30.2	29.6	30.1	30.4	29.6	30.0	29.7	30.0	30.1	29.6	30.2	30.2
0.28	0.80	0.40	0.19	0.63	0.44	0.72	0.52	0.53	0.69	0.30	0.37
6.46	16.2	18.2	6.52	12.8	10.6	19.2	19.5	18.1	21.4	14.8	17.3
8.02	1.38	2.22	6.47	2.51	3.79	2.82	2.23	4.49	2.31	7.19	6.67
2.88	2.53	2.02	2.11	4.31	4.66	2.87	2.42	2.42	2.68	2.62	3.04
9.42	5.79	9.35	12.6	7.63	7.43	6.15	5.36	6.50	5.29	6.29	5.38
21.9	20.1	19.6	23.5	20.6	20.7	18.1	17.4	17.6	16.5	18.1	16.3
2.35	2.64	1.91	2.21	2.50	2.45	2.12	2.32	2.19	2.17	2.03	1.96
8.76	10.4	7.22	7.76	9.21	9.05	7.97	8.95	7.50	7.38	6.83	6.37
2.47	3.38	1.90	2.11	2.55	2.57	2.52	3.21	2.33	2.85	2.63	2.63
2.17	1.98	1.40	1.69	2.51	2.49	2.06	2.28	1.80	2.38	1.94	2.09
0.32	0.12	0.13	0.28	0.34	0.39	0.28	0.30	0.30	0.24	0.29	0.32
0.63	0.61	0.60	0.70	1.14	1.29	0.84	0.81	0.75	0.88	0.88	1.10
0.09	0.04	0.05	0.04	0.15	0.14	0.07	0.05	0.18	0.05	0.06	0.09
0.19	0.26	0.17	0.06	0.36	0.36	0.23	0.13	0.23	0.21	0.16	0.21
0.03	0.08	0.03	—	0.03	0.05	0.04	—	0.04	0.04	0.02	0.02
3.15	3.29	4.23	2.77	2.87	2.91	4.19	4.21	4.46	4.70	4.83	5.07
0.46	0.34	0.38	0.38	0.27	0.30	0.38	0.38	0.43	0.35	0.50	0.51
99.7	99.6	100.0	99.7	100.0	99.7	100.3	100.1	100.0	99.7	99.6	99.5
0.011	0.031	0.016	0.007	0.024	0.017	0.028	0.020	0.020	0.027	0.012	0.014
0.634	0.600	0.565	0.681	0.598	0.594	0.520	0.525	0.509	0.483	0.504	0.459
0.103	0.092	0.072	0.079	0.147	0.156	0.104	0.096	0.092	0.104	0.096	0.111
0.252	0.276	0.348	0.232	0.231	0.234	0.348	0.356	0.379	0.386	0.388	0.415

TABLE 1—*Extended*

	Group C Li-mica S-type granites									Group D Li-mica *A*-type granites	
	Cheralite-(Ce)							Brabantite		Mon-(Ce)	Cher-(Ce)
Granite	POB	POB	EIB	POB	G4	EIB	G4	EIB	EIB	SEI	SEI
Sample	911-F	910-F	819-F	910-F	4194	507-F	4194	819-F	239-F	1056	1056
Mineral host	Li-mica	quartz	quartz	quartz	quartz	Li-mica	feldspar	quartz	Li-mica	quartz	quartz
Analysis	25	26	27	28	29	30	31	32	33	34	35
P_2O_5	29.9	30.2	30.1	30.2	30.2	30.1	30.1	30.6	29.6	30.5	29.5
SiO_2	0.58	0.39	0.41	0.35	0.42	0.33	0.45	0.26	0.71	0.19	0.75
ThO_2	20.9	23.8	25.2	25.6	35.9	38.8	40.5	40.9	51.7	0.23	18.4
UO_2	3.56	2.27	2.45	4.57	3.45	4.04	3.12	5.26	2.07	—	0.74
Y_2O_3	3.14	2.44	2.19	2.39	2.05	2.09	2.28	1.29	0.18	2.23	1.24
La_2O_3	4.79	4.12	4.20	4.77	2.99	3.11	2.15	2.09	—	14.3	8.37
Ce_2O_3	15.5	13.9	14.5	11.6	7.69	6.40	6.30	4.70	—	29.8	20.9
Pr_2O_3	2.07	1.98	1.98	1.40	0.89	0.61	0.57	0.47	—	3.17	2.29
Nd_2O_3	7.39	6.66	6.47	5.42	2.96	2.36	2.07	1.89	—	13.3	8.44
Sm_2O_3	3.06	3.56	2.91	2.20	1.15	0.81	0.93	0.61	n.a.	2.62	2.29
Gd_2O_3	2.43	2.56	1.90	2.01	1.18	0.97	1.20	0.89	n.a.	2.04	1.84
Tb_2O_3	0.31	0.38	0.18	0.22	0.19	0.09	0.30	0.08	n.a.	0.22	0.18
Dy_2O_3	1.06	0.93	0.64	0.74	0.73	0.72	0.80	0.40	—	0.61	0.79
Ho_2O_3	0.07	0.11	n.a.	0.10	0.05	n.a.	0.06	n.a.	n.a.	0.13	0.06
Er_2O_3	0.19	0.18	0.09	0.20	0.18	0.16	0.21	0.22	n.a.	0.15	0.25
Yb_2O_3	0.02	0.06	0.02	0.03	0.03	0.05	0.02	—	—	0.02	0.05
CaO	4.77	5.69	5.85	6.75	8.28	8.91	8.87	9.94	11.4	0.28	3.50
PbO	0.44	0.44	0.51	0.58	0.63	n.d.	0.66	0.89	0.98	0.01	0.27
Total	100.2	99.5	99.6	99.1	98.9	99.5	100.6	100.5	96.6	99.8	99.9
Mole fractions											
$ThSiO_4$	0.022	0.015	0.016	0.014	0.016	0.013	0.017	0.010	0.004	0.002	0.029
$(La\text{-}Sm)PO_4$	0.461	0.422	0.423	0.356	0.221	0.187	0.168	0.136		0.890	0.602
$Y,(Gd\text{-}Lu)PO_4$	0.117	0.103	0.081	0.091	0.072	0.068	0.079	0.046	0.004	0.086	0.067
$(Th,Ca,U,Pb)[PO_4]_2$	0.400	0.458	0.480	0.539	0.690	0.732	0.735	0.808	0.968	0.018	0.301

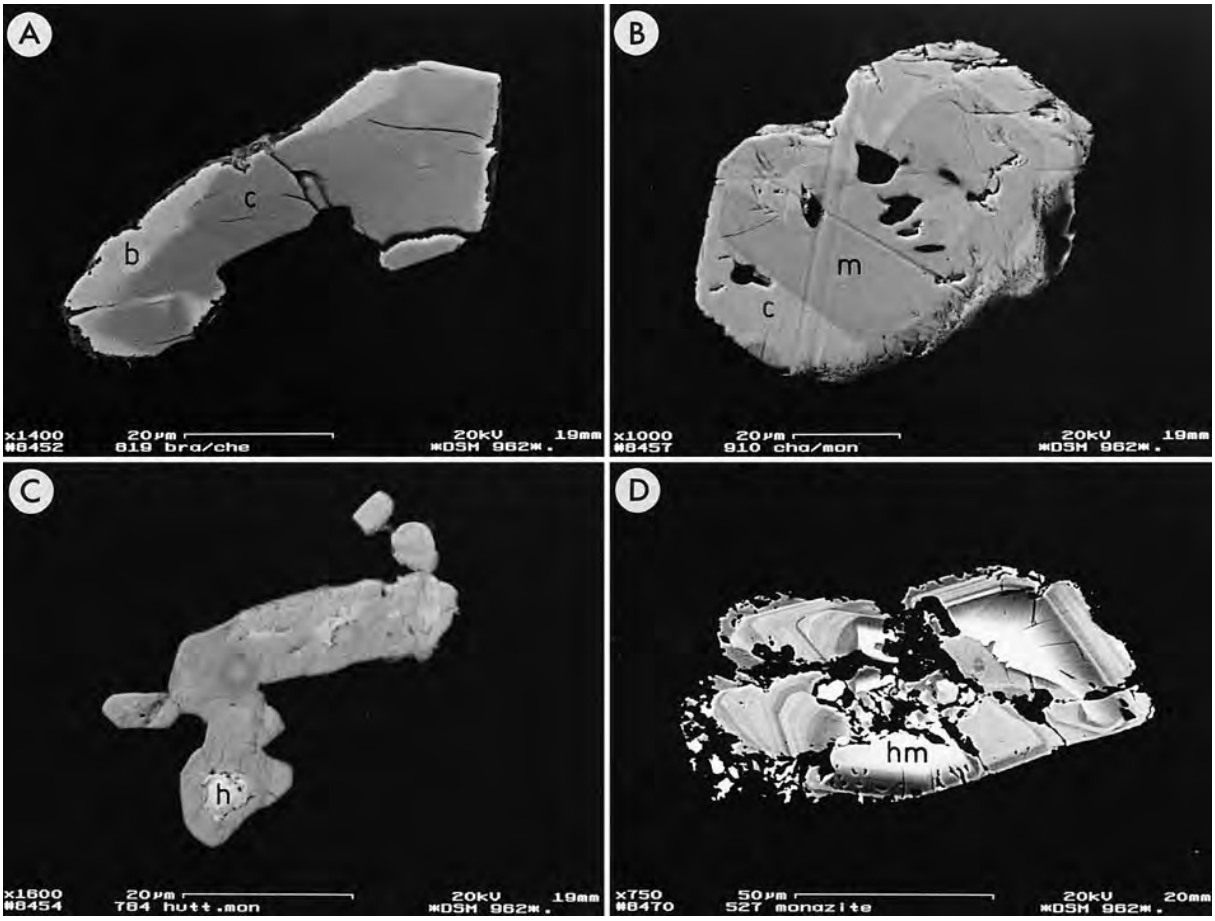

FIGURE 2. Backscattered scanning electron microscope images of Th-rich monazite group minerals. (**A)** brabantite (point b; Table 1, analysis 32) rimming cheralite-(Ce) (point c; Table 1, analysis 27). (**B)** cheralite-(Ce) (Table 1, analysis 26) forming a rim on zoned monazite (m). (**C)** huttonitic monazite-(Ce) (h; Table 1, analysis 8) in Th-rich monazite. (**D)** huttonite-rich monazite-(Ce) (hm; Table 1, analysis 11) in the center of a complexly zoned, corroded monazite. The BSE images were recorded with different beam current and different gain of the photomultiplier to optimize the resolution for each grain. Areas of similar chemical composition thus do not have the same gray tone in the different BSE pictures.

squares) plot almost perfectly along the vector representing the brabantite substitution, $Ca(Th,U)REE_{-2}$. However, a few of the analyses (marked by filled triangles) plot very close to the vector that indicates the huttonite substitution, $(Th,U)SiREE_{-1}P_{-1}$.

The extent of huttonite substitution in monazite ranges from zero to 42.6 mol%. Huttonite-rich monazite-(Ce) was discovered in transitional I-S type biotite and two-mica granites (Table 1, analyses 4, 5, 16), and also occurs in the biotite granites of A-type affinity (14.3 wt% ThO_2 or 13.3 mol% $Th(U)SiO_4$ at a maximum). At its upper extreme, compositions extended well into the field of huttonitic monazite (Table 1, analysis 8) outlined in this paper (see Fig. 6b). This particular huttonitic monazite-(Ce) contains some fluorine (0.35 wt%), and it is also perhaps slightly hydrated, considering its relatively low analytical total of ~99 wt%. This composition is similar to the huttonitic monazites from pegmatites in Poland (see Fig. 6a) described by Kucha (1980) and may result from weak metamictization.

Cheralite-(Ce) is most common in the S-type Li-mica granites, including the massifs of Eibenstock, Pobershau, and Satzung in the Erzgebirge (Table 1, analyses 19–21, 25–28, 30) and the G4 intrusion in the Fichtelgebirge (Table 1, analyses 22–24, 29, 31). Cheralite-(Ce) is not restricted to this granite group, however, but also occurs in biotite granite (Kirchberg; Table 1, analyses 10–11), two-mica granite (Schwarzenberg, Lauter, G1S; Table 1, analyses 13–15), and Li-mica A-type granite (Seiffen; Table 1, analysis 35). On the other hand, brabantite was found exclusively in the S-type Li-mica granites (Table 1, analyses 32–33). The brabantite represented by analysis 32 is even closer to the theoretical end-member composition than is the type brabantite from Namibia (see Figs. 6a and 6b).

Uranium. Concentrations of UO_2 in granitic monazites

rarely exceed 1 wt% (Cuney and Friedrich 1987). Table 1 lists several analyses with U concentrations in monazite-(Ce), cheralite-(Ce), and brabantite that are among the highest values reported to date. To the author's knowledge, the cheralite-(Ce) from the G1S granite sample 11389, which has 8 wt% UO_2 (analysis 13), is only exceeded in U content by one from an U-rich leucogranite from Albuquerque, Spain (Bea 1996), which contains 13.8 wt% UO_2. Granitic pegmatites are the only environment from which similar or higher U concentrations, e.g., 9.5 wt% UO_2 (Gulson and Krogh 1973) and 15.6 wt% UO_2 (Gramaccioli and Segelstad 1978), have been reported in minerals of this group. Uranium enrichment is not necessarily accompanied by an enrichment in thorium, however. Average monazite-(Ce) typically shows a strong preference for Th over U, resulting in Th/U $\geq$ 10. In contrast, several analyses shown in Table 1 document unusual Th/U close to or below 1 (analyses 12, 13, 16). Similarly, low Th/U ratios between 1.6 and 1, coupled with high UO_2 concentrations (5.9 to 7.1 wt%), have been reported for late magmatic monazites from the St. Sylvestre peraluminous granite in the French Massif Central (Friedrich and Cuney 1989).

REE. Typical reported concentrations of Nd_2O_3 in monazite-(Ce) from granitic rocks are between 8 and 12 wt%. This study revealed a number of monazite-(Ce) minerals that have substantially higher Nd contents (Table 1, analyses 3–5). Nd enrichment is generally accompanied by enhanced contents of Sm_2O_3 up to 5.3 wt%. Within composite granite plutons, aplites are the preferential hosts of monazite-(Ce) enriched in Nd and Sm (e.g., Wark and Miller 1993). The highest content of Nd in monazite-(Ce) from this study (21.5 wt% Nd_2O_3) was found in a fine-grained (aplitic?) granite from Schlema-Alberoda (Table 1, analysis 5). This is the highest concentration reported in a monazite-group mineral from a granitic rock and is surpassed in the literature only by hydrothermal monazite-(Nd) from a fissure at Glogstafelberg in the Alps, which contain 29.7 wt% Nd_2O_3 and 9.4 wt% Sm_2O_3 (Graeser and Schwander 1977). Other examples of Nd-rich monazite-(Ce) occur in peraluminous granites from Spain (18.8 wt% Nd_2O_3; Casillas et al. 1995) and Russia (18.3 wt% Nd_2O_3; Bea 1996), the Gloserheia granitic pegmatite in southern Norway (up to 20.8 wt% Nd_2O_3; Åmli 1975), low-grade metapelitic schists from NE Bavaria, Germany (up to 19.1 wt% Nd_2O_3; Heinrich et al. 1997), and calc-silicate rocks from Ontario, Canada (up to 16.9 wt% Nd_2O_3; Pan 1997).

Some monazite grains (Table 1, analyses 17, 18) were found in which the concentration of Y greatly exceeds that described in average natural monazite (0.5 to 2.5 wt% Y_2O_3). Y_2O_3 contents >4 wt% are found in monazite-(Ce) from two-mica granites as well as Li-mica granites, and these are among the highest values reported so far. Cheralite-(Ce) also contains high concentrations of Y_2O_3, between 2 and 3 wt%.

Except for Gd, published analytical data for the HREE in monazite are limited, irrespective of lithology, which makes it difficult to establish typical concentration ranges for the HREE in monazites from granitic rocks. The highest Gd_2O_3 content in the present study is 3.5 wt%, from a monazite-(Ce) in aplite of the Kirchberg biotite granite pluton (Table 1, analysis 3). Concentrations of Gd_2O_3 exceeding 2 wt% are found in most of the cheralites-(Ce), but these are not unusual for monazites from granitic rocks. However, it seems safe to conclude that Tb_2O_3 concentrations close to 0.4 wt% and Dy_2O_3 concentrations of 1.3 wt%, which are found in a Y-rich monazite-(Ce) from the Eibenstock S-type Li-mica granite pluton (Table 1, analysis 18), are uncommonly high values. Of the heavier HREE, only Er may be present in appreciable amounts, even up to a few tenths of a weight percent Er_2O_3 (Table 1, analyses 12, 17, 18).

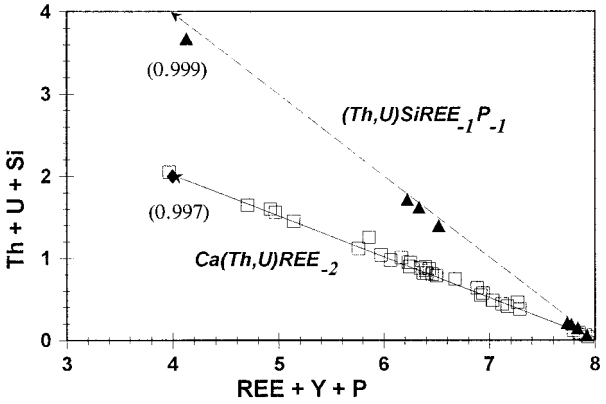

FIGURE 3. A plot of formula proportions (Th + U + Si) vs. (REE + Y + P) calculated on the basis of 16 O atoms. Monazite-group minerals in which the molar abundance of the huttonite molecule exceeds that of the brabantite molecule are marked by filled triangles. Open squares represent those for which brabantite exceeds huttonite (see Table 1). The dashed arrow represents the huttonitic substitution, the solid arrow the brabantitic substitution. The correlation coefficients (R) for the best fit regression for the huttonite and brabantite-dominated monazite-group minerals, respectively, are given in parentheses.

Representative chondrite-normalized (CN) REE patterns of the monazite-group minerals are shown in Figures 4 and 5. These figures reveal that monazites show considerable variability in the shapes of their REE patterns. Monazites particularly rich in brabantite typically possess flat LREE patterns (Fig. 4a), whereas those very poor in Th may show very steep patterns (Fig. 4b). Many of the cheralites-(Ce) display characteristic LREE patterns with discontinuities at La and Nd (Fig. 4a, analyses 11 and 26; Fig. 5). Flat patterns also characterize monazites with atypically low Th/U, as well as those rich in Nd and Sm (Fig. 4b). An excellent example of the variability in the shapes of the REE patterns is given by the most Nd-rich monazite-(Ce), which is distinguished by a convex-upward curved segment between La and Sm and a local maxima at Pr (Fig. 4b, analysis 5).

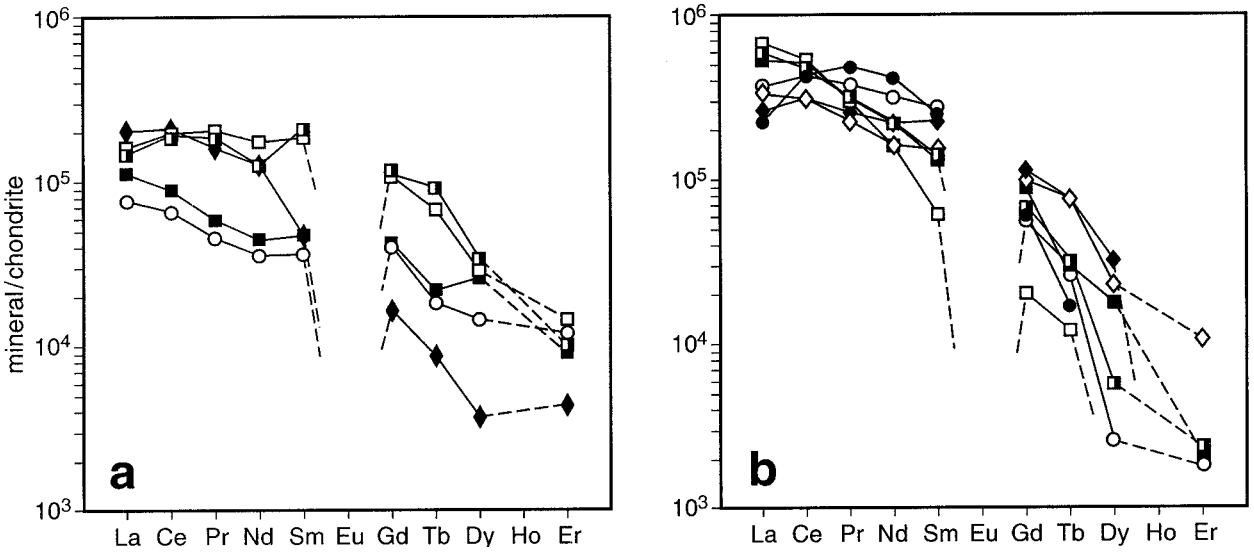

FIGURE 4. Representative chondrite-normalized REE patterns of monazite-group minerals from the Erzgebirge-Fichtelgebirge granites. Compositional data are compiled from Table 1. **(a)** Th-rich minerals: huttonitic monazite-(Ce) = filled diamonds (analysis 8); cheralite-(Ce) = open squares (analysis 7), half-filled squares (analysis 28), and filled squares (analysis 30); brabantite = open circles (analysis 32). **(b)** monazite-(Ce) or cheralite-(Ce) either very poor in Th (open squares, analysis 10; half-filled squares, analysis 9; filled squares, analysis 1), rich in Nd (open circles, analysis 4; dots, analysis 5), or having U/Th ratios >1 (open diamonds, analysis 13; filled diamonds, analysis 18). Chondritic REE abundances used here and in Figure 5 are taken from Anders and Grevesse (1989).

Granite compositions and correlations with monazite type

Table 2 reports the whole-rock chemical compositions of the granites that contain huttonitic monazite-(Ce), cheralite-(Ce), and brabantite. These granites are all silica-rich (>73.5 wt% SiO_2), strongly fractionated (TiO_2 < 0.13 wt%) rocks that display relatively flat LREE patterns ($La_N/Sm_N < 3$).

Cheralite-(Ce) has been identified preferentially, and brabantite exclusively, in F- and P-rich, S-type Li-mica granites that are substantially depleted in LREE, Th, and Y, but enriched in U (see below). Furthermore, these rocks are distinguished by fractionated, non-chondritic ratios of the geochemically similar element pairs Y-Ho and Zr-Hf, and some display the lanthanide tetrad effect (e.g., Förster and Tischendorf 1994; Bau 1996; Irber et al. 1997). The concentrations of Th, Y, and the HREE in both monazite-group minerals and their host group C granites are inversely correlated.

However, as shown in the previous section, the occurrence of cheralite-(Ce) is not restricted to strongly peraluminous S-type granites. This mineral also has been identified in the other groups of granites that include rocks with low F and P and moderate to high LREE, Th, and Y concentrations (Table 2).

DISCUSSION

Nomenclature and examples of the monazite-brabantite-huttonite isotructural series

Monazite forms part of an isostructural series of monoclinic minerals with the general formula ABO_4, where A = REE, Y, Th, U, Ca, Pb and B = P, Si. Because La, Ce, and Nd are typically the dominant LREE in natural monazites, we follow the proposal of the IMA in distinguishing the members monazite-(La), monazite-(Ce), and monazite-(Nd). Huttonite ($ThSiO_4$-Pabst and Hutton 1951)

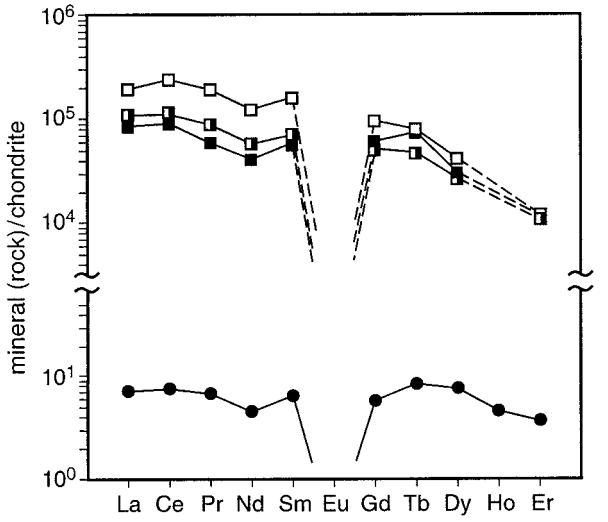

FIGURE 5. Comparison of the shapes of chondrite-normalized La-Er patterns of cheralite-(Ce) (open squares = analysis 24; half-filled squares = analysis 29; filled squares = analysis 31) and their host granite (G4 in the Fichtelgebirge, sample 4194). The whole-rock REE concentrations are from Irber et al. (1997).

TABLE 2. Geochemistry of huttonitic monazite-(Ce), cheralite-(Ce), and brabantite-bearing granites

Pluton	KIB, aplite	KIB, aplite	LAU	SWB	SZU	EIB	EIB	EIB	POB	EIB	POB	G4	SEI
Granite group	A	A	B	B	C	C	C	C	C	C	C	C	D
Sample	784	1073	807	803	930	239	814	507	910	819	911	*4194	1056
†Monazite type	h, c	c	c	c	c	c	c	c, b	c	c, b	c	c	c
La	7.50	2.11	4.16	3.23	6.55	3.66	4.36	3.32	3.74	2.70	1.90	1.69	18.2
Ce	17.2	5.32	8.33	6.67	15.4	8.99	10.4	7.90	9.17	6.39	4.91	4.50	46.4
Pr	2.34	0.72	1.00	0.78	1.92	1.18	1.26	1.00	1.20	0.73	0.63	0.59	6.14
Nd	8.86	2.73	3.49	2.56	6.85	3.98	4.49	3.75	4.27	2.70	2.17	2.00	21.4
Sm	3.48	1.01	0.90	0.85	2.07	1.27	1.45	1.18	1.47	0.97	0.98	0.93	6.34
Eu	0.07	0.04	0.07	0.02	0.08	0.02	0.05	0.04	0.05	0.002	0.009	0.005	0.24
Gd	4.03	1.05	0.80	0.77	2.12	1.38	1.51	1.11	1.71	0.94	1.11	1.12	6.25
Tb	0.87	0.24	0.16	0.20	0.45	0.30	0.34	0.28	0.41	0.29	0.28	0.30	1.33
Dy	5.99	1.57	1.05	1.16	2.85	1.87	2.04	1.68	2.41	1.76	1.66	1.82	9.21
Ho	1.25	0.30	0.20	0.20	0.46	0.30	0.32	0.27	0.36	0.25	0.21	0.25	1.90
Er	4.25	1.02	0.70	0.68	1.19	0.77	0.80	0.74	0.81	0.78	0.47	0.58	5.36
Tm	0.66	0.18	0.13	0.13	0.16	0.12	0.11	0.10	0.10	0.11	0.06	0.08	1.16
Yb	4.54	1.46	1.00	1.18	1.04	0.74	0.66	0.66	0.58	0.78	0.36	0.50	8.86
Lu	0.68	0.21	0.16	0.18	0.14	0.09	0.09	0.11	0.07	0.10	0.04	0.06	1.33
Y	33.7	10.5	6.7	7.3	15.2	10.2	10.7	10.0	12.7	9.2	7.8	9.2	55.2
Th	22.5	4.1	4.6	4.5	11.0	7.1	7.4	6.7	8.4	6.4	5.5	7.5	24.4
U	56.3	14.5	5.3	10.3	34.9	11.3	8.5	12.2	42.1	11.4	30.0	20.5	17.9
A/CNK‡	1.08	0.99	1.24	1.23	1.23	1.26	1.24	1.22	1.21	1.31	1.29	1.32	1.19
SiO_2	77.1	73.8	76.6	76.0	75.0	74.9	74.6	74.4	75.2	73.9	74.4	74.6	73.7
TiO_2	0.054	0.060	0.062	0.056	0.085	0.065	0.072	0.057	0.057	0.046	0.042	0.030	0.121
P_2O_5	0.060	0.256	0.117	0.180	0.293	0.321	0.396	0.415	0.308	0.436	0.388	0.270	0.063
F	0.017	0.048	0.075	0.097	0.486	0.732	0.685	0.687	0.298	0.859	0.665	0.520	0.638
Sum La-Sm	39.42	11.89	17.88	14.09	32.79	19.08	21.96	17.15	19.85	13.49	10.59	9.71	98.48
La_N/Sm_N	1.35	1.31	2.90	2.38	1.98	1.81	1.88	1.76	1.59	1.74	1.21	1.14	1.80
Y/Ho	27.0	35.0	33.4	36.5	32.9	34.5	33.4	34.8	35.3	36.8	37.3	36.8	29.1
Zr/Hf	20.4	13.1	17.6	14.8	25.5	23.0	22.2	19.2	21.1	17.9	18.4	15.8	16.7

Note: Trace elements in parts per million; oxides and F in weight percents.
* The data for sample 4194 are from Hecht (1993) and Irber et al. (1997).
† Monazite type: h = huttonitic monazite-(Ce); c = cheralite-(Ce); b = brabanite.
‡ A/CNK = molar $Al_2O_3/(Na_2O + K_2O + CaO)$.

and brabantite [$CaTh(PO_4)_2$-Rose 1980] are the other prominent end-members. The name cheralite-(Ce) [(LREE,Ca,Th,U)(P,Si)O_4-Bowie and Horne 1953; Hughes et al. 1995] is applied to members intermediate in composition between monazite and brabantite. The species boundaries in the ternary system 2 $CePO_4$-$CaTh(PO_4)_2$−2 $ThSiO_4$ proposed by Bowie and Horne (1953) are shown in Fig. 6a (see Burt 1989, Fig. 10, for a vector-based version of this diagram). This plot also shows the compositions of Th-rich monazite-group minerals known prior to this study.

The type locality of huttonite is Gillespie's Beach, New Zealand, where it occurs as minute grains in beach sand (Pabst and Hutton 1951). Wet chemical analyses revealed 76.6 wt% ThO_2. The name huttonite is also used for minerals from granitic pegmatites of Bogatynia, Poland, (Kucha 1980) that are intermediate in composition (ThO_2 = 56.4 to 69.9 wt%) between $ThSiO_4$ and $CePO_4$. The latter plot in an unnamed field of the classification diagram of Bowie and Horne (1953) and Rose (1980) (cf. Fig. 6a) and, therefore, cannot be considered as huttonite sensu stricto. Because there is no established name for this region of the diagram, we propose the term *huttonitic monazite* for minerals plotting between monazite and huttonite. Poitrasson et al. (1996) reported a hydrothermally altered monazite containing 28.9 wt% ThO_2 from the Skiddaw granite, northwest England; according to the current proposal, this is a huttonitic monazite. The same holds for a mineral from a holocrystalline ejectum from Vetralla, Italy, and a mineral from a metapelitic granulite from Strona, Italy, which have 27.1 wt% ThO_2 (della Ventura et al. 1996) and 27.3 wt% ThO_2 (Bea 1996). The latter author described various Th-orthosilicates in granitic rocks, which he suggested may represent unaltered huttonite and intermediate monazite-huttonite phases. The latter minerals are highly non-stoichiometric and show a predominance of HREE over LREE, suggesting that they may represent non-metamict thorites or intermediate members of the thorite-xenotime solid solution series. Additional occurrences of huttonitic monazite are described in Speer (1980).

Brabantite has been only noted twice in the literature and was found exclusively in granitic pegmatites. The type mineral from the Brabant farm, Namibia, contains 54.7 wt% ThO_2 (Rose 1980). Wet chemical analyses of the brabantite from Xingjiang, China, gave 51.1 wt% ThO_2 and 1.52 wt% (UO_2 + UO_3) (Xianjue 1978, cited in Fleischer et al. 1981).

Cheralite-(Ce) was first discovered in the Kuttakuzhi granite pegmatite, India, by Bowie and Horne (1953), and the type mineral contains 31.6 wt% ThO_2 (Bowles et al. 1980). Other occurrences include Xinjiiang, China (Hughes et al. 1995), Bogatynia, Poland (Kucha 1980), and three granitic pegmatites of the Alps (minerals con-

taining up to 23.6 wt% ThO_2 and 15.6 wt% UO_2; Gramaccioli and Segalstad 1978; Mannucci et al. 1986; Demartin et al. 1991). A ThO_2-rich (21.6 wt%) and strongly altered monazite from the Carnmenellis granite, southwest England (Poitrasson et al. 1996), as well as an U-rich (13.4 wt% UO_2) monazite from a two-mica leucogranite from Albuquerque, Spain (Bea 1996), are technically also cheralites-(Ce) according to the scheme shown in Figure 6a.

Thorium and uranium substitutions

The incorporation of the actinides in the monazite-group minerals presented in this paper occurs by almost pure huttonite or brabantite substitution (see Fig. 3). In contrast, substitution of these elements in ''common'' monazite can be described by an approximately equal contribution of both the above components (van Emden et al. 1997; see also Franz et al. 1996).

As documented in Table 2, the amount of thorium found in monazite is virtually independent of the Th content of the granitic melt, assuming that the latter can be approximated by the Th content in the bulk-rock. For uranium, Podor et al. (1995) showed experimentally that there is no crystal-chemical limit to U substitution in monazite at *P-T* conditions corresponding to those of granite crystallization. The initial availability of U in the melt was invoked by these authors as one factor controlling the amount of U incorporated into monazite. In the Erzgebirge in particular, it appears that U was mobile, and that the highly variable and, in some cases low, U contents listed in Table 2 are not representative of the primary values. Tischendorf and Förster (1994) showed that leaching by fluids of non- magmatic origin caused significant U loss, particularly from two-mica and Li-mica granites, and the fluids locally gave rise to large vein-type U deposits. Undisturbed high initial U abundances, close to the saturation limit in peraluminuous melts, are best displayed by the Pobershau and Satzung granites, which on average contain 30 to 40 ppm U and low Th/U between 0.1 and 1 (see Table 2). However, the monazite-(Ce), cheralite-(Ce), or brabantite that formed in these exceptionally U-rich granites of group C typically possess only low to medium U contents (see Table 1) and high Th/U (mostly between 10 and 20). Evolved granite differentiates of the Kirchberg biotite granite suite have between 25 and 30 ppm U (Förster and Tischendorf 1994) but contain monazite-(Ce) with UO_2 concentrations commonly much less than 1 wt% (Förster and Rhede 1995). Therefore, U-rich silicate magmas do not necessarily crystallize U-rich monazites. Apparently, U^{4+} shows a strong tendency to form uraninite (present in all groups of granites discussed here) or uranothorite (present only in biotite and F-rich A-type granites) rather than substituting preferentially into monazite or xenotime.

Conditions of mineral formation

It is beyond the scope of this paper to discuss in detail the mechanisms and processes that caused the compositional extremes in the monazite group minerals presented here. We emphasize that 95% of the monazite in these rocks is of ''normal'' composition.

Compositional and textural relationships suggest that a variety of open- and closed-system processes operated during different stages of magmatic evolution, but these are not understood fully (e.g., Wark and Miller 1993). This complexity is manifested, for example, in the occurrence of compositionally dissimilar monazite-group minerals such as ''normal'' monazite-(Ce), huttonitic monazite-(Ce), cheralite-(Ce), and Th-poor, Nd-rich monazite-(Ce) in a single thin section of one of the aplites related to the Kirchberg granite pluton (Table 1, analyses 4, 7, 8). The compositional heterogeneity observed is probably related to REE-phosphate supersaturation, perhaps accompanying the breakdown of previous REE-bearing phases. It is possible that monazite grains having strongly different compositions could form simultaneously in such circumstances and persist together either stably or metastably in response to gradients in the activity of selected species in the melt or fluid. For example, Pan (1997) noted the simultaneous formation of Th-poor and Th-rich monazites in aluminous gneiss by the breakdown of pre-existing REE- and Th-bearing minerals (titanite and zircon). Diffusion-controlled compositional gradients in the regions adjacent to growing major phases and the growing accessory crystal itself, as proposed by Wark and Miller (1993), is another plausible mechanism to explain the formation of Th-rich rims on or as patchy zones within crystals of lower Th content.

The time when the monazite-group minerals formed during magmatic evolution is uncertain. In principle, they could represent either early to late equilibrium magmatic phases, early to late disequilibrium metasomatic phases, or fragments of restite. Biotite-hosted, very low-Th monazites-(Ce) with steep LREE profiles might (without further evidence) represent good candidates for early formed igneous minerals or, perhaps, inherited phases. On the other hand, the unusual REE pattern (e.g., Fig. 4b), amoeboid shape, and interstitial (late) position of the most Nd-rich monazite-(Ce) can be explained best by precipitation from residual solutions that penetrated through the host granite during the early hydrothermal stage.

The Th(U)-rich members of the monazite group are particularly well suited for dating by the chemical Th-U-total Pb method (Rhede et al. 1996, and references therein). Application of this method yielded Variscan ages for all the actinide-rich minerals studied here, in agreement with the isotopically constrained ages of their granite hosts. No pre-Variscan ages were obtained, which argues against a restitic origin of these phases. There is also no indication that they formed as a result of incongruent dissolution of apatite during late magmatic evolution as demonstrated experimentally by Wolf and London (1995). Nevertheless, some of these monazite grains, and more likely a greater part of the ''normal'' varieties, may have formed by such incongruent dissolution at or near

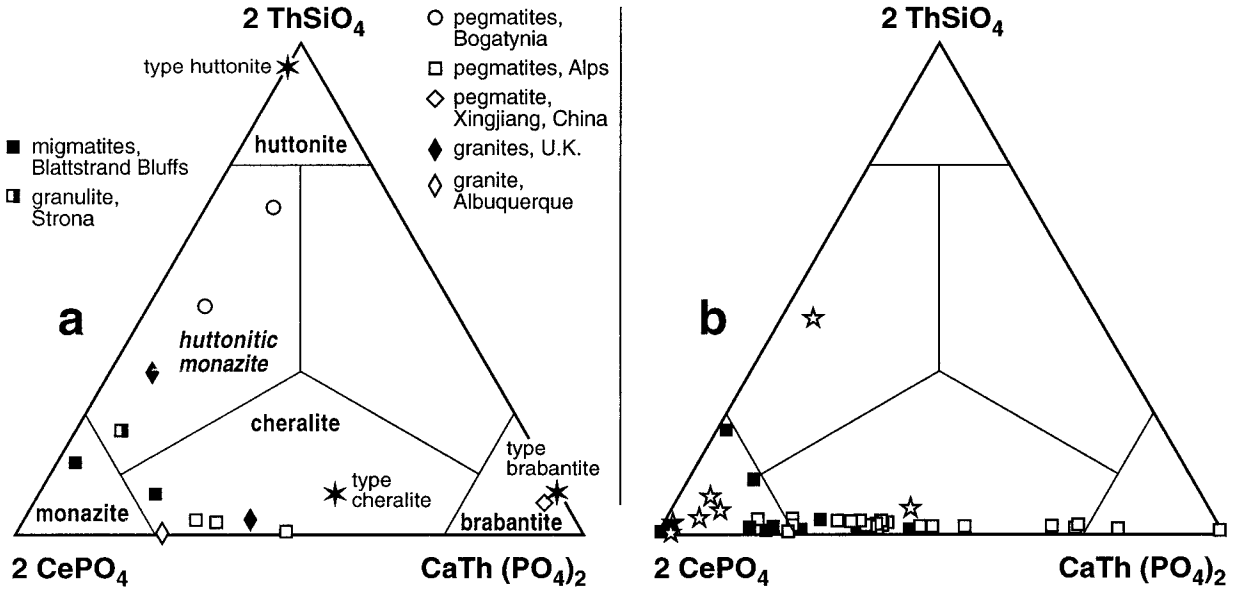

FIGURE 6. Nomenclature of the system 2 $CePO_4$-$CaTh(PO_4)_2$–2 $ThSiO_4$ (Bowie and Horne 1953). In calculating end-member proportions, the contents of other REE and Y are added to Ce, and the contents of U and Pb are included with the brabantite molecule. **(a)** Type brabantite (Rose 1980), type huttonite (Pabst and Hutton 1951), type cheralite (Bowles et al. 1980), Bogatynia (Kucha 1980), Alpine pegmatites (Cantadore and Gramaccioli 1968; Gramaccioli and Segelstad 1978; Manucci et al. 1986), Carnmenellis and Skiddaw granites from the U.K. (Poitrasson et al. 1996), Albuquerque (Bea 1996), Blattstrand Bluffs (Watt 1995), Strona (Bea 1996). **(b)** Compositions of monazite-group minerals from granites of the Erzgebirge-Fichtelgebirge, Germany; stars = biotite granites, filled squares = two-mica granites, open squares = Li-mica S-type granites. See text for further explanations.

the site of melting, and may have separated from the parental phase during ascent of the magma.

Cheralite-(Ce), brabantite, and many of the other Th-rich monazites-(Ce) appear to represent late-stage phenomena rather than early formed magmatic minerals. They are closest in composition to minerals precipitated from pegmatitic melts (see Rapp and Watson 1986, and references therein). In fact, residual granitic melts from the Erzgebirge are extraordinarily evolved, being variably enriched in Li, Rb, Cs, B, and F. These melts had low solidus temperatures, ranging from about 650 to 580 °C (Thomas et al. 1996), similar to pegmatite-forming liquids (Webster et al. 1997).

Furthermore, some of these minerals typically display discontinuous chondrite-normalized LREE patterns (e.g., downward kinks at La and Nd: Figs. 4 and 5). These irregularities have been attributed to the lanthanide tetrad effect (see Bau 1996). The origin of this pattern in minerals and bulk rocks is disputed (McLennan 1994). Yurimoto et al. (1990) argued that the kink at Nd in the LREE pattern of evolved S-type leucogranites and pegmatites can be explained by fractional crystallization involving monazite. The depletion of La relative to Ce, however, cannot be produced by Rayleigh fractionation of monazite (Bau 1997). In agreement with Bau (1996), we prefer a model involving differential complexation of REE in highly evolved, ligand-rich granitic magmas transitional between silicate melts and hydrothermal fluids. Fluid-rich residual liquids are favorable environments for crystallization of the rare members of the monazite group.

Monazite crystals can also be affected by high-temperature dissolution (some of the crystals analyzed here are embayed and corroded). Reaction with volatile-rich residual silicate liquids or solutions may release some Th, which could reprecipate to form the Th-rich rims or domains. Most of the granites under consideration here show evidence of variable overprinting, as follows: secondary chlorite, sericite, muscovite ± fluorite in biotite granites; muscovite ± fluorite, apatite, and tourmaline in two-mica granites; and zinnwaldite, muscovite, apatite, topaz ± fluorite in Li-mica granites. None of the cheralites-(Ce) and brabantites analyzed here occur within or on phases that can be identified unambiguously as secondary. These minerals do not share the combination of textural and compositional features that characterize hydrothermally altered, Th-rich phases from granites described by Jefferies (1985), Ward et al. (1992), and Poitrasson et al. (1996). However, the huttonite-rich monazite-(Ce) (Table 1, analysis 8), which forms an irregular domain in the center of a magmatically zoned, cracked and corroded monazite grain (e.g., Fig. 2D) that is surrounded by chloritized biotite, probably formed due to alteration.

IMPLICATIONS

This study demonstrates for the first time that brabantite may precipitate from granitic melts. It also reports

many new occurrences of cheralite-(Ce) as well as a monazite-group mineral intermediate between monazite-(Ce) and huttonite, for which the term huttonitic monazite is proposed in extension of the nomenclature introduced by Bowie and Horne (1953). The study also documents an extensive compositional diversity in monazite-(Ce) with respect to the actinide and lanthanide elements.

Highly differentiated, strongly peraluminous, low-temperature residual melts of S-type affinity, which are rich in fluorine and other volatile constituents but depleted in Th and the LREE, appear particularly likely to crystallize brabantite. The Eibenstock granite constitutes the third reported occurrence worldwide of this rare member of the monazite group. Such volatile-rich liquids, from which this granite crystallized, share many features in common with pegmatitic melts.

Cheralite-(Ce) may be present in highly evolved, silica-rich granites that differ greatly in their concentrations of REE, Th, U, and Y as well as P and F. This suggests that the total lanthanide and actinide concentrations in monazite and host granite are correlated only poorly (or not at all), and that neither fluorine nor phosphorus alone are crucial for the formation of the Th-rich monazite-group minerals.

''Irregular'' LREE patterns with anomalies at La or Nd (or both) are characteristic of many of the brabantite-rich monazite-group minerals. In an exceptional case, where cheralite-(Ce) is more abundant than ''common'' monazite, this mineral governs the shape of the discontinuous LREE pattern of the host rock (see Fig. 5). In contrast, crystals of monazite-(Ce) that are found in more primitive granites, or that appear to have formed earlier than other Th-rich phases, possess regular LREE patterns. To understand better the formation conditions of the various monazite-group minerals, and to overcome the existing uncertainties in defining the points in time during magmatic history at which they may form, additional experimental work on the stability of the individual monazite-group minerals is needed.

The monazites studied here span almost the entire compositional range previously recorded in the monazite-(Ce)-brabantite-huttonite ternary system. The compositional data provide evidence for complete miscibility in the monazite-(Ce)-brabantite solid solution series under natural conditions, as assumed by Rose (1980) and Bea (1996). Miscibility was recently demonstrated experimentally by Podor and Cuney (1997) at *P-T* conditions corresponding to those of granitic magmas (780 °C, 200 Mpa). The monazite-(Ce)-huttonite join is less completely occupied by natural minerals, but some of these are from granites. In contrast, the substitution $2\ Th^{4+}(U^{4+}) + Si^{4+} \leftrightarrow Ca^{2+} + 2\ P^{5+}$ (brabantite-huttonite join) appears to be lacking in monazite-group minerals in granites.

Finally, the compositional diversity shown here for monazite-group minerals in granites has important implications for trace-element fractionation modeling. Workers who attempt quantitative modeling of monazite fractionation should consider the internal variability of accessory mineral compositions even in a single grain or thin section, and the relations of monazite composition with the host granite chemistry. Even if relevant data on monazite chemistry were available, because the REE, Y, Th, and U are hosted preferentially in accessories, they are not suitable elements for petrogenetic modeling of granitoids using equilibrium-based fractionation models (e.g., Bea 1996).

Acknowledgments

The author thanks Dieter Rhede and Oona Appelt, Potsdam, for their invaluable assistance in the electron microprobe work and their tireless efforts to develop optimal analytical conditions. I am particularly grateful to Gerhard Tischendorf (Berlin) who, over the past several years, participated in all field campaigns during which the Erzgebirge granite samples were collected, and who offered valuable ideas on granite genesis and evolution. This part of the work dealing with monazite-group minerals from the Fichtelgebirge was financially supported by the Deutsche Forschungsgemeinschaft (DFG, grant Mo 232/24, 1-2). Lutz Hecht (München) kindly provided powdered rock samples from the Fichtelgebirge granites for ICP-MS analyses performed by Peter Dulski (Berlin). This work benefited from careful journal reviews and valuable suggestions by George B. Morgan VI (Norman) and Donald M. Burt (Tempe). F. Poitrasson (Toulouse) is acknowledged for sharing his ideas on the genesis of Th-rich monazite in granites from the U.K. Finally, Robert Trumbull (Potsdam) is thanked for critically reading and improving a first draft of this manuscript.

References cited

Åmli, R. (1975) Mineralogy and rare earth geochemistry of apatite and xenotime from the Gloserheia granite pegmatite, Froland, southern Norway. American Mineralogist, 60, 607–620.

Åmli, R. and Griffin, W.L. (1975) Microprobe analysis of REE minerals using empirical correction factors. American Mineralogist, 60, 599–606.

Anders, E. and Grevesse, N. (1989) Abundances of the elements: meteoritic and salor. Geochimica et Cosmochimica Acta, 53, 197–214.

Bau, M. (1996) Controls on the fractionation of isovalent trace elements in magmatic and aqueous systems: Evidence from Y/Ho, Zr/Hf, and lanthanide tetrad effect. Contributions to Mineralogy and Petrology, 123, 323–333.

——— (1997) The lanthanide tetrad effect in highly evolved felsic igneous rocks—a reply to the comment by Y. Pan. Contributions to Mineralogy and Petrology, 128, 409–412.

Bea, F. (1996) Residence of REE, Y, Th and U in granites and crustal protoliths; Implications for the chemistry of crustal melts. Journal of Petrology, 37, 521–552.

Bea, F., Pereira, M.D., Corretge, L.G., and Fershtater, G.B. (1994) Differentiation of strongly peraluminous, perphosphorous granites: The Pedrobernardo pluton, central Spain. Geochimica et Cosmochimica Acta, 58, 2609– 2627.

Boatner, L.A. and Sales, B.C. (1988) Monazite. In W. Lutze and R.C. Ewing, Eds., Radioactive Waste Forms for the Future, p. 495–564. Elsevier, Amsterdam.

Bowie, S.H.U. and Horne, J.E.T. (1953) Cheralite, a new mineral of the monazite group. Mineralogical Magazine, 30, 93–99.

Bowles, J.F.W., Jobbins, E.A., and Young, B.R. (1980) A re-examination of cheralite. Mineralogical Magazine, 43, 885–888.

Breiter, K., Sokolova, M., and Sokol, A. (1991) Geochemical specialization of the tin-bearing granitoid massifs of NW Bohemia. Mineralium Deposita, 26, 298–306.

Burt, D.M. (1989) Compositional and phase relations among rare earth element minerals. In Mineralogical Society of America Reviews in Mineralogy, 21, 259–307.

Casillas, R., Nagy, G., Pantó, G., Brändle, J., and Fórizs, I. (1995) Occurrence of Th, U, Y, Zr, and REE- bearing accessory minerals in late-Variscan granitic rocks from the Sierra de Guadarrama (Spain). European Journal of Mineralogy, 7, 989–1006.

Charoy, B. and Pollard, P.J. (1989) Albite-rich, silica-depleted metasomatic rocks at Emuford, northeast Queensland: Mineralogical, geochemical, and fluid inclusion constraints on hydrothermal evolution and tin mineralization. Economic Geology, 84, 1850–1874.

Cuney, M. and Friedrich, M. (1987) Physicochemical and crystal-chemical controls on accessory mineral paragenesis in granitoids: Implications for uranium metallogenesis. Bulletin Minéralogie, 110, 235–247.

Cuney, M., Le Fort, P., and Wang, Z.X. (1984) Uranium and thorium geochemistry and mineralogy in the Manaslu leucogranite (Nepal, Himalaya). In Xu Keqin and Tu Guangchi, Eds., Geology of Granites and their Metallogenetic Relations, p. 853–873. Proceedings of the International Symposium, Nanjing, China, University Sciences Editions.

Della Ventura, G., Mottana, A., Parodi, G.C., Raudsepp, M., Bellatreccia, F., Caprilli, E., Rossi, P., and Fiori, S. (1996) Monazite-huttonite solid-solutions from the Vico Volcanic Complex, Latium, Italy. Mineralogical Magazine, 60, 751–758.

Demartin, F., Pilati, T., Diella, V., Donzelli, S., and Gramaccioli, C.M. (1991) Alpine monazite: further data. Canadian Mineralogist, 29, 61–67.

Drake, M.J. and Weill, D.F. (1972) New rare earth elements standards for electron microprobe analysis. Chemical Geology, 10, 179–181.

Dulski, P. (1994) Interferences of oxide, hydroxide, and chloride analyte species in the determination of rare earth elements in geological samples by inductively coupled plasma-mass spectrometry. Fresenius Journal of Analytical Chemistry, 350, 194–203.

van Emden, B., Thornber, M.R., Graham, J., and Lincoln, F.J. (1997) The incorporation of actinides in monazite and xenotime from placer deposits in western Australia. Canadian Mineralogist, 35, 95–104.

Exley, R.A. (1980) Microprobe studies of REE-rich accessory minerals: Implications for Skye granite petrogenesis and REE mobility in hydrothermal systems. Earth and Planetary Science Letters, 48, 97–110.

Fleischer, M., Chao, G.Y., and Francis, C.A. (1981) New mineral names. American Mineralogist, 66, 878–879.

Förster, H.-J. and Rhede, D. (1995) Extreme compositional variability in granitic monazites. U.S. Geological Survey Circular Abstracts, 1129, 54–55.

Förster, H.-J., Seltmann, R., and Tischendorf, G. (1995) High-fluorine, low-phosphorus A-type (post-collision) silicic magmatism in the Erzgebirge. In 2nd Symposium on Permocarboniferous Igneous Rocks, Extended Abstracts. Terra Nostra, 7, 32–35.

Förster, H.-J. and Tischendorf, G. (1994) The western Erzgebirge-Vogtland granites: Implications to the Hercynian magmatism in the Erzgebirge-Fichtelgebirge anticlinorium. In R. Seltmann, H. Kämpf, and P. Möller, Eds., Metallogeny of Collisional Orogens, p. 35–48. Czech Geological Survey, Prague.

Franz, G., Andrehs, G., and Rhede, D. (1996) Crystal chemistry of monazite and xenotime from Saxothuringian-Moldanubian metapelites, NE Bavaria, Germany. European Journal of Mineralogy, 8, 1097–1118.

Friedrich, M.H. and Cuney, M. (1989) Uranium enrichment processes in peraluminous magmatism. In Uranium Deposits in Magmatic and Metamorphic Rocks, IAEA-TC-571/2, p. 11–35. International Atomic Energy Agency, Vienna.

Graeser, S. and Schwander, H. (1977) Gasparite-(Ce) and monazite-(Nd): Two new minerals to the monazite group from the Alps. Schweizer Mineralogische und Petrographische Mitteilungen, 67, 103–113.

Gramaccioli, C.M. and Segalstad, T.V. (1978) A uranium- and thorium-rich monazite from a south-alpine pegmatite at Piona, Italy. American Mineralogist, 63, 757–761.

Gulson, B.L. and Krogh, T.E. (1973) Old lead component in the young Bergell Massif, south-east Swiss Alps. Contributions to Mineralogy and Petrology, 40, 239–252.

Harrison, T.M., McKeegan, K.D., and Le Fort, P. (1995) Detection of inherited monazite in the Manaslu leucogranite by $^{208}Pb/^{232}Th$ ion microprobe dating: Crystallization age and tectonic implications. Earth and Planetary Science Letters, 133, 271–282.

Hecht, L. (1993) Die Glimmer als Indikatoren für die magmatische und postmagmatische Entwicklung der Granite des Fichtelgebirges (NE-Bayern). p. 221, Münchner Geologische Hefte.

Hecht, L., Vigneresse, J.L., and Morteani, G. (1997) Constraints on the origin and zonation of the granite complexes in the Fichtelgebirge (Germany and Czech Republic): Evidence from a gravity and geochemical study. Geologische Rundschau, 86, Supplement, S93–S109.

Heinrich, W., Andrehs, G., and Franz, G. (1997) Monazite-xenotime miscibility gap thermometer: 1. An empirical calibration. Journal of Metamorphic Geology, 15, 3–16.

Hinton, R.W. and Paterson, B.A. (1994) Crystallisation history of granitic magma: Evidence from trace element zoning. Mineralogical Magazine, 58A, 416–417.

Hughes, J.M., Foord, E.E., Hubbard, M.A., and Ni, Y. (1995) The crystal structure of cheralite-(Ce), (LREE, Ca, Th, U)(P, Si)O_4, a monazite-group mineral. Neues Jahrbuch für Mineralogie Monatshefte, No. 8, 344–350.

Irber, W., Förster, H.-J., Hecht, L., Möller, P., and Morteani, G. (1997) Experimental, geochemical, mineralogical, and stable isotope constraints on the late-magmatic history of the Fichtelgebirge granites (Germany). Geologische Rundschau, 86, Supplement, S110–S124.

Jarosewich, E. and Boatner, L.A. (1991) Rare-earth element reference samples for electron microprobe analysis. Geostandards Newsletter, 15, 397–399.

Jefferies, N.L. (1985) The distribution of the rare earth elements within the Carnmenellis pluton, Cornwall. Mineralogical Magazine, 49, 495–504.

Jennings, J.A. and Rowbotham, G. (1995) The composition of accessory mineral phases with possible petrogenetic implications for the Hercynian granites of north-west Finestère, Brittany, France. Proceedings of the Ussher Society, 8, 387–393.

Johan, Z. and Johan, V. (1993) Accessory minerals of the Cínovec granitic cupola; Behaviour of REE in F- and CO_2-rich fluids. In F. Fenoll Hach-Ali, J. Torres-Ruiz, and F. Gervilla, Eds., Current Research in Geology Applied to Ore Deposits, p. 625–628. La Guioconda, Granada.

Kucha, H. (1980) Continuity in the monazite-huttonite series. Mineralogical Magazine, 43, 1031–1034.

Mannucci, G., Diella, V., Gramaccioli, C.M., and Pilati, T. (1986) A comparative study of some pegmatitic and fissure monazite from the Alps. Canadian Mineralogist, 24, 469–474.

Maruéjol, P., Cuney, M., and Turpin, L. (1990) Magmatic and hydrothermal R.E.E. fractionation in the Xihuashan granites (SE China). Contributions to Mineralogy and Petrology, 104, 670–688.

McLennan, S.M. (1994) Rare earth element geochemistry and the ''tetrad'' effect. Geochimica et Cosmochimica Acta, 58, 2025–2033.

Miller, C.F., Hanchar, J.M., Wooden, J.L., Bennett, V.C., Harrison, T.M., Wark, D.A., and Foster, D.A. (1992) Source region of a granite batholith: Evidence from lower crustal xenoliths and inherited accessory minerals. Transactions of the Royal Society of Edinburgh, Earth Sciences, 83, 49–62.

Montel, J.-M. (1993) A model for monazite/melt equilibrium and application to the generation of granitic magmas. Chemical Geology, 110, 127–146.

Montel, J.-M., Foret, S., Veschambre, M., Nicollet, C. and Provost, A. (1996) Electron microprobe dating of monazite. Chemical Geology, 131, 37–53.

Nabelek, P.I. and Glascock, M.D. (1995) REE-depleted leucogranites, Black Hills, South Dakota: A consequence of disequilibrium melting of monazite-bearing schists. Journal of Petrology, 36, 1055–1071.

Pabst, A. and Hutton, C.O. (1951) Huttonite, a new monoclinic thorium silicate with an account on its occurrence, analysis, and properties. American Mineralogist, 36, 60–69.

Pan, Y. (1997) Zircon- and monazite-forming metamorphic reactions at Manitouwadge, Ontario. Canadian Mineralogist, 35, 105–118.

Parrish, R.R. (1990) U-Pb dating of monazite and its application to geological problems. Canadian Journal of Earth Sciences, 27, 1431–1450.

Podor, R. and Cuney, M. (1997) Experimental study of Th-bearing $LaPO_4$ (780 °C, 200 MPa): Implications for monazite and actinide orthophosphate stability. American Mineralogist, 82, 765–771.

Podor, R., Cuney, M., and Nguyen Trung, C. (1995) Experimental study of the solid solution between monazite-(La) and $(Ca_{0.5}U_{0.5})PO_4$ at 780 °C and 200 MPa. American Mineralogist, 80, 1261–1268.

Poitrasson, F., Chenery, S., and Bland, D.J. (1996) Contrasted monazite hydrothermal alteration mechanisms and their geochemical implications. Earth and Planetary Science Letters, 145, 79–96.

Pouchou, J.L. and Pichoir, F. (1985) ''PAP'' (ø-ρ-*Z*) procedure for improved quantitative microanalysis. In J.T. Armstrong, Ed., Microbeam Analysis, p. 104–106. San Francisco Press, California.

Rapp, R.P. and Watson, E.B. (1986) Monazite solubility and dissolution kinetics: Implications for the thorium and light rare earth chemistry of felsic magmas. Contributions to Mineralogy and Petrology, 94, 304–316.

Rapp, R.P., Ryerson, F.J., and Miller, C.F. (1987) Experimental evidence bearing on the stability of monazite during crustal anatexis. Geophysical Research Letters, 14, 307–310.

Rhede, D., Wendt, I. and Förster, H.-J. (1996) A three-dimensional method for calculating independent chemical U/Pb- and Th/Pb-ages of accessory minerals. Chemical Geology, 130, 247–253.

Roeder, P.L. (1985) Electron-microprobe analysis of minerals for rare-earth elements: use of calculated peak-overlap corrections. Canadian Mineralogist, 23, 263–271.

Rose, D. (1980) Brabantite, $CaTh[PO_4]_2$, a new mineral of the monazite group. Neues Jahrbuch für Mineralogie Monatshefte, 247–257.

Speer, J.A. (1980) The actinide orthosilicates. In Mineralogical Society of America Reviews in Mineralogy, 5, 113–135.

Suzuki, K., Adachi, M. and Kajizuka, I. (1994) Electron microprobe observations of Pb diffusion in metamorphosed detritical monazites. Earth and Planetary Science Letters, 128, 391–405.

Thomas, R., Rhede, D., and Trumbull, R.B. (1996) Microthermometry of volatile-rich silicate melt inclusions in granitic rocks. Zeitschrift für geologische Wissenschaften, 24, 505–526.

Tischendorf, G. and Förster, H.-J. (1994) Hercynian granite magmatism and related metallogenesis in the Erzgebirge: A status report. In K.V. Gehlen and D.D. Klemm, Eds., Mineral Deposits of the Erzgebirge/Krušné hory (Germany/Czech Republic). Monograph Series on Mineral Deposits, 31, 5–23.

Ward, C.D., McArthur, J.M., and Walsh, J.N. (1992) Rare earth element behavior during evolution and alteration of the Dartmoor granite, SW England. Journal of Petrology, 33, 785–815.

Wark, D.A. and Miller, C.F. (1993) Accessory mineral behavior during differentiation of a granite suite: Monazite, xenotime, and zircon in the Sweetwater wash pluton, southeastern California, U.S.A. Chemical Geology, 110, 49–67.

Watt, G.R. (1995) High-thorium monazite-(Ce) formed during disequilibrium melting of metapelites under granulite-facies conditions. Mineralogical Magazine, 59, 735–743.

Watt, G.R. and Harley, S.L. (1993) Accessory phase control on the geochemistry of crustal melts and restites produced during water-undersaturated partial melting. Contributions to Mineralogy and Petrology, 114, 550–566.

Webster, J.D., Thomas, R., Rhede, D., Förster, H.-J., and Seltmann, R. (1997) Melt inclusions in quartz from an evolved peraluminous pegmatite: Geochemical evidence for strong tin enrichment in fluorine- and phosphorus-rich residual liquids. Geochimica et Cosmochimica Acta, 61, 2589–2604.

Wolf, M.D. and London, D. (1995) Incongruent dissolution of REE- and Sr-rich apatite in peraluminous granitic liquids: Differential apatite, monazite, and xenotime solubilities during anatexis. American Mineralogist, 80, 765–775.

Yurimoto, H., Duke, E.F., Papike, J.J. and Shearer, C.K. (1990) Are discontinuous chondrite-normalized REE patterns in pegmatitic granite systems the results of monazite fractionation? Geochimica et Cosmochimica Acta, 54, 2141– 2145.

Zhao, J.-X. and Cooper, J.A. (1993) Fractionation of monazite in the development of V-shaped REE patterns in leucogranite systems: Evidence from a muscovite leucogranite body in central Australia. Lithos, 30, 23–32.

Manuscript received April 9, 1997
Manuscript accepted November 10, 1997